



Effect of the magnetic field on the nonlinear optical rectification and second and third harmonic generation in double δ -doped GaAs quantum wells

J.C. Martínez-Orozco^{a,*}, J.G. Rojas-Briseño^{a,b}, K.A. Rodríguez-Magdaleno^{a,b}, I. Rodríguez-Vargas^{a,b}, M.E. Mora-Ramos^b, R.L. Restrepo^c, F. Ungan^d, E. Kasapoglu^e, C.A. Duque^f

^a Unidad Académica de Física, Universidad Autónoma de Zacatecas, Calzada Solidaridad esquina con Paseo la Bufa S/N, C.P. 98060 Zacatecas, Zac, Mexico

^b Centro de Investigación en Ciencias, Instituto de Investigación en Ciencias Básicas y Aplicadas, Universidad Autónoma del Estado de Morelos, Av. Universidad 1001, CP 62209 Cuernavaca, Morelos, Mexico

^c Universidad EIA, CP 055428 Envigado, Colombia

^d Faculty of Technology, Department of Optical Engineering, Cumhuriyet University, 58140 Sivas, Turkey

^e Faculty of Science, Department of Physics, Cumhuriyet University, 58140 Sivas, Turkey

^f Grupo de Materia Condensada-UdeA, Instituto de Física, Facultad de Ciencias Exactas y Naturales, Universidad de Antioquia UdeA, Calle 70 No. 52-21, Medellín, Colombia

ARTICLE INFO

Keywords:

δ -doped QW
Nonlinear optical rectification
Second Harmonic Generation
Third Harmonic Generation

ABSTRACT

In this paper we are reporting the computation for the Nonlinear Optical Rectification (NOR) and the Second and Third Harmonic Generation (SHG and THG) related with electronic states of asymmetric double Si- δ -doped quantum well in a GaAs matrix when this is subjected to an in-plane (x -oriented) constant magnetic field effect. The work is performed in the effective mass and parabolic band approximations in order to compute the electronic structure for the system by a diagonalization procedure. The expressions for the nonlinear optical susceptibilities, $\chi_0^{(2)}$, $\chi_{2\omega}^{(2)}$, and $\chi_{3\omega}^{(3)}$, are those arising from the compact matrix density formulation and stand for the NOR, SHG, and THG, respectively. This asymmetric double δ -doped quantum well potential profile actually exhibits nonzero NOR, SHG, and THG responses which can be easily controlled by the in-plane (x -direction) externally applied magnetic field. In particular we find that for the chosen configuration the harmonic generation is in the far-infrared/THz region, thus and becoming suitable building blocks for photodetectors in this range of the electromagnetic spectra.

1. Introduction

Nowadays it is well known that the quantum confinement of the charge carriers in low-dimensional semiconductor structures -electrons or holes- is of great importance for the development of optoelectronic devices [1]. In particular, for one dimensional (1D) confining potential profiles there has been a significant amount of proposed potential profiles that are experimentally feasible thanks to modern and sophisticated semiconductor growth techniques [2]. Among the different structures designed with these 1D-potential profiles we can mention some studies on nonlinear optical (NLO) properties that include linear and nonlinear absorption coefficients [3–7], nonlinear optical rectification (NOR) as well as second and third harmonic generation. Many works have been reported dealing with single and multiple rectangular quantum wells (QWs) [8–15], parabolic and semi-parabolic QWs [16–21], and Pöschl-Teller QWs [22]. In general, any desired potential profile can be obtained due to the high-control over the experimental

semiconductor growth techniques [23]. For the NOR, the first experimental report for asymmetrical quantum dot (QD) was performed by Rosencher et al. [24]. Related to the second harmonic generation (SHG), it is possible to find in the literature reports on: i) SHG controlled via an externally applied electric field [25], ii) high-quality AlGaAs nanoantennas as a source of preferential direction of SHG [26], iii) that the SHG can be substantially enhanced in compositional asymmetrical QWs [27], and iv) that the SHG has been theoretically analyzed in correlation with intersubband (ISB) transitions in QWs made with two-dimensional periodic metamaterials [28]. On the other hand, there are also some studies related to the third harmonic generation (THG). For instance Wang et al. [29] reported the THG for asymmetric coupled rectangular $\text{Al}_x\text{Ga}_{1-x}\text{As}/\text{GaAs}$ QWs and Zhang and Xie [30] studied this property in a semi-parabolic QW with an applied electric field. Finally, Ganguly et al. [31] recently reported a meticulous analysis of the third-order nonlinear optical susceptibility for an impurity-doped QDs by considering a magnetic field as a

* Corresponding author.

E-mail address: jcmartinez@uaz.edu.mx (J.C. Martínez-Orozco).

confinement source and a static applied electric field. In general, this kind of intersubband transitions are suitable as photodetectors, for instance in the mid-infrared [32] and in the far-infrared [33], and the δ -doping profile is an alternative to design this kind of devices.

In the particular case of δ -doped-like potential profiles, there are also some recent studies in NLO properties [34–44]. For instance, Ozturk and Sökmen [34] performed the ISB optical absorption coefficient computation, by means of a self-consistent procedure, for a symmetric double Si- δ -doped quantum well in a GaAs matrix in presence of an external electric field, applied along the growth direction. Posteriorly, Ozturk [35] reported the ISB optical absorption coefficient taking into account the influence of an in-plane magnetic field, also for the symmetric case configuration. More recently, Rodríguez-Magdaleno et al. [41] reported the ISB-related nonlinear optical absorption coefficient and relative refractive index change for an asymmetric double δ -doped QW potential profile with the inclusion of an externally applied electric field. In the case of single and double QWs, G. Gumbs used the self-consistent density of states computation to investigate the energy spectrum as a function of an externally applied magnetic field [45].

In this paper, we report for the first time the NOR, SHG, and THG for an asymmetric double Si- δ -doped GaAs QW subject to the influence of an in-plane (x -oriented) constant magnetic field effect. The calculations are carried out within the effective mass and parabolic band approximations and optical properties are treated using the compact matrix density formulation. The organization of the paper is as follows: Section 2 contains the description of the theoretical model. In Section 3 we discuss the corresponding results. Finally, Section 4 presents the main conclusions of the study.

2. Theoretical framework

Here, we are using the effective mass and parabolic band approximations to obtain the energy level spectrum of an asymmetric double Si- δ -doped GaAs quantum well (DDQW) as a function of an in-plane (x -directed) constant magnetic field. For this particular configuration, in the Landau gauge, the vector potential is $\vec{A} = -Bz\hat{y}$, resulting in the Hamiltonian,

$$\frac{1}{2m_e^*} \left[-\hbar^2 \nabla^2 - 2q\hbar i B z \frac{\partial}{\partial y} + q^2 B^2 z^2 \right] + V_{qw}(z), \quad (1)$$

that commutes with the momentum operators \hat{p}_x and \hat{p}_y . Then, the wave function of the system can be proposed as written as:

$$\Psi(x, y, z) = \psi(z) e^{i k_x x + i k_y y}, \quad (2)$$

where $\psi(z)$ satisfies the equation

$$\left[-\frac{\hbar^2}{2m_e^*} \frac{d}{dz} + \frac{(qB)^2}{2m_e^*} \left(z + \frac{\hbar k_y}{qB} \right)^2 + V_{qw}(z) \right] \psi(z) = \left(E - \frac{\hbar^2 k_x^2}{2m_e^*} \right) \psi(z). \quad (3)$$

In the case of $k_x = k_y = 0$, the equation to solve is

$$\left[-\frac{\hbar^2}{2m_e^*} \frac{d}{dz} + \frac{(qB)^2}{2m_e^*} z^2 + V_{qw}(z) \right] \psi(z) = E\psi(z). \quad (4)$$

In these expressions, m_e^* represents the electron effective mass ($=0.067 m_0$), $q = -e$ (being e the absolute value of the electron charge), and B stands for the magnetic field strength. The one-dimensional self-consistent potential $V_{qw}(z)$ represents the confinement potential profile generated by the double δ -doped quantum well. Using the Thomas-Fermi approximation [46], the potential associated to the δ -layers is given by:

$$V_{qw}(z) = -\frac{\alpha^2}{(\alpha|z - l_p/2| + z_0^l)^4} - \frac{\alpha^2}{(\alpha|z + l_p/2| + z_0^r)^4}, \quad (5)$$

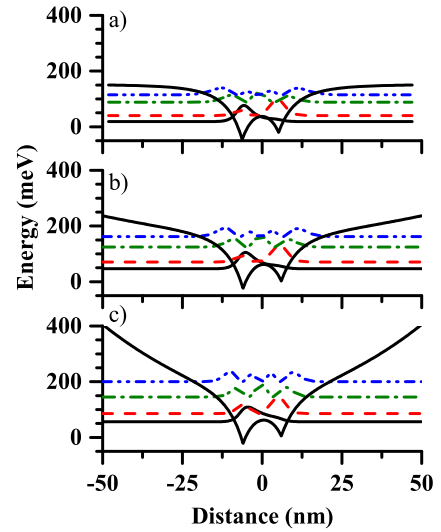


Fig. 1. Potential profile for an asymmetric double δ -doped quantum well for a) zero applied magnetic field, b) $B = 10$ T, and c) $B = 20$ T. In each case the probability densities for the first four confined states are also depicted, schematically.

where $\pm l_p/2$ represents the semi-distance -measured from the origin- for the left- and right-hand δ -doped quantum well minima. The other potential model parameters that appear in the previous equation are:

$$\alpha = \frac{e^2 m_e^*{}^{3/2}}{15 \pi \epsilon_r \hbar^3} \quad \text{and} \quad z_0^{l,r} = \left(\frac{\alpha^3 m_e^*{}^{3/2}}{15 \pi^2 \epsilon_r \hbar^3 N_{2d}^{l,r}} \right)^{1/5}, \quad (6)$$

here ϵ_r is the GaAs static dielectric constant, N_{2d}^l (N_{2d}^r) represents the two-dimensional ionized impurity density for the left-hand (right-hand) side of the δ -doped layer. The remaining parameters are well known physical quantities.

The method used to solve the Schrödinger equation associated to the Hamiltonian given by the Eq. (3) with a confining potential (see Fig. 1) is the diagonalization procedure, which consists in proposing an expansion of the envelope function in terms of a complete set of orthonormal functions

$$\psi(z) = \sum_{m=1}^{\infty} c_m \phi_m(z). \quad (7)$$

In general, any complete set of orthonormal functions ($\langle \phi_m(z) | \phi_n(z) \rangle = \delta_{m,n}$) satisfies this basic quantum mechanical property. Nevertheless, for a practical implementation of the method we must restrict the summation to a finite value (n_p). This means that choosing a suitable basis also plays a role in reducing the number of terms included. In the case under study the expansion basis chosen are the analytical solutions of an infinite-confinement-potential one-dimensional QW, centered at the origin, having a width L_∞

$$\phi_m(z) = \left(\frac{2}{L_\infty} \right)^{1/2} \sin \left(\frac{m \pi z}{L_\infty} + \frac{m \pi}{2} \right). \quad (8)$$

In this particular computation we have used $n_p = 50$ and $L_\infty = 100$ nm, which ensures the convergence for the computed energy levels emerging as the eigenvalues of the Hamiltonian matrix H_{mn} ($H_{mn} = \langle \phi_m(z) | H(z) | \phi_n(z) \rangle$). In order to validate our results we have reproduced previous Poisson-Schrödinger self-consistent results finding good agreement with the energy differences for the symmetric case reported by E. Ozturk [35]. As mentioned, we deal with the more general asymmetric case. Actually, it is more difficult to solve self-consistently; hence we believe that our procedure can be rather advantageous. Once the whole electronic structure is calculated we care able to compute the dipole matrix elements that allows us to obtain the desired optical properties.

For the computation of the optical nonlinearities in asymmetric

QWs, the study follows the lines of Rosencher and Bois [47], making use of the so-called compact matrix density. This later quantity obeys the Von Neumann's equation of motion

$$\frac{\partial \hat{\rho}_{ij}}{\partial t} = \frac{1}{i\hbar} [\hat{H}_0 - \hat{M} E(t), \hat{\rho}]_{ij} - \Gamma_{ij} (\hat{\rho} - \hat{\rho}^{(0)})_{ij}, \quad (9)$$

where $\hat{\rho}^{(0)}$ is the unperturbed density matrix and \hat{H}_0 is the unperturbed Hamiltonian of the system (without considering the incident electromagnetic field $E(t)$). Γ_{ij} represents the relaxation rate that phenomenologically accounts for damping in the system, and \hat{M} is the electric dipole moment operator. As it is known, for the relaxation rates we define: $\Gamma_1 = 1/T_1$ for the inelastic relaxation rate (associated to lifetime of diagonal terms, $i = j$) and $\Gamma_2 = 1/T_2$ for the elastic relaxation rate ($i \neq j$). The Eq. (9) can be solved by means of an iterative method [47].

The electronic polarization $P(t)$ can be expanded in terms of the electric field series as follows

$$P(t) = \varepsilon_0 \chi_{\omega}^{(1)} \tilde{E} e^{i\omega t} + \varepsilon_0 \chi_{\omega}^{(2)} |\tilde{E}|^2 + \varepsilon_0 \chi_{2\omega}^{(2)} \tilde{E}^2 e^{2i\omega t} + \varepsilon_0 \chi_{\omega}^{(3)} |\tilde{E}|^2 \tilde{E} e^{i\omega t} + \varepsilon_0 \chi_{3\omega}^{(3)} \tilde{E}^3 e^{3i\omega t} + c. c., \quad (10)$$

where ε_0 is the permittivity of the free space. In this study we are interested in the calculation of the coefficients of the Nonlinear Optical Rectification $\chi_{\omega}^{(2)}$, the Second Harmonic Generation $\chi_{2\omega}^{(2)}$, and Third Harmonic Generation $\chi_{3\omega}^{(3)}$ contributions.

For the evaluation of the NOR-coefficient we shall only consider the main energy transition (from ground state to the first excited state), the corresponding coefficient is given by [47]

$$\chi_{\omega}^{(2)} = \frac{4e^3 \rho_{01} M_{01}^2 \delta_{01}}{\varepsilon_0 \hbar^2} \frac{\omega_{10}^2 \left(1 + \frac{\Gamma_2}{\Gamma_1}\right) + (\omega^2 + \Gamma_2^2) \left(\frac{\Gamma_2}{\Gamma_1} - 1\right)}{(\omega_{10} - \omega)^2 + \Gamma_2^2 [(\omega_{10} + \omega)^2 + \Gamma_2^2]}, \quad (11)$$

with $\rho_{01} = \rho_0 - \rho_1$ being ρ_i the concentration of charge carriers for the i -th subband. Besides, $\delta_{01} = M_{11} - M_{00}$, whilst $M_{01} = \langle \psi_0(z) | z | \psi_1(z) \rangle$ is the main transition dipole matrix element.

For the SHG and THG to be possible, the energy level structure must consist of at least three and four levels with equal spacing, respectively. These are requirements that fulfills only approximately in quantum well systems, although the possibility of tuning the spectrum of levels by means of geometrical or compositional settings may always lead to an almost homogeneous distribution of energy differences, fundamentally for symmetric quantum well potentials. Nonetheless Rosencher and Bois [47] deduced expressions that allowed us to calculate the coefficient corresponding to the SHG in the case of non-symmetric QWs

$$\chi_{2\omega}^{(2)} = \frac{e^3 \rho_{01}}{\varepsilon_0 \hbar^2} \frac{M_{01} M_{12} M_{20}}{(\omega_{10}^{(1)} - i\Gamma_1)(\omega_{20}^{(2)} - i\Gamma_2)}. \quad (12)$$

For the coefficient of THG, Shao et al. [48] reported that

$$\chi_{3\omega}^{(3)} = \frac{e^4 \rho_{03}}{\varepsilon_0 \hbar^3} \frac{M_{01} M_{12} M_{23} M_{30}}{(\omega_{10}^{(1)} + i\Gamma_1)(\omega_{20}^{(2)} + i\Gamma_2)(\omega_{30}^{(3)} + i\Gamma_3)}, \quad (13)$$

with $\omega_{10}^{(1)} = \omega - \omega_{10}$, $\omega_{20}^{(2)} = 2\omega - \omega_{20}$ and $\omega_{30}^{(3)} = 3\omega - \omega_{30}$. The parameter that appears in these equations are $\omega_{ji} = (E_j - E_i)/\hbar$ and $M_{ij} = \int \phi_j^*(z) z \phi_i(z) dz$. In addition, the quantity $\rho_{0i} = \rho_0 - \rho_i$ ($i = 1, 3$), appearing in Eqs. (11)–(13), are the 3D concentration for the electrons in the levels involved in the transition.

Here we deal with quantum states where the interval of energy between them depends of the physical parameters of the structure. However, we are interested in the triple resonance, which corresponds to $\omega = \omega_{10} = \omega_{20}/2 = \omega_{30}/3$. Consequently, our Eq. (13) corresponds to the same approximation used by Yuan et al. [49] for the type-I combination of the levels that they took into account for the calculations of the THG (compare Eqs. (12) and (13) in Ref. [49] with the Eq. (13) in the present manuscript). It is worth mentioning that this is, in fact, a reduced form of the complete mathematical expression for $\chi_{3\omega}^{(3)}$

(see, for instance, Ref. [30] that includes only the full resonant term and neglects those contributing with lesser amplitudes).

The concentration of charge carriers for the i -th subband has been obtained via the expression

$$\rho_i = \frac{m_e^* k_B T}{\pi \hbar^2 L_{\infty}} \ln \left[1 + \exp \left(\frac{E_F - E_i}{k_B T} \right) \right], \quad (14)$$

where E_i is the energy of the corresponding subband, T is the temperature, k_B is the Boltzmann constant, and E_F is the Fermi energy. In the low temperature regime ($T \simeq 4$ K) the previous equation can be approximated to $\rho_i = \frac{m_e^*}{\pi \hbar^2 L_{\infty}} (E_F - E_i)$ and the difference of concentration of carriers between two levels ($\rho_{ij} = \rho_i - \rho_j$) is given by $\rho_{ij} = \frac{m_e^*}{\pi \hbar^2 L_{\infty}} (E_j - E_i)$.

3. Results and discussion

Let us now present and discuss the results obtained for the NOR as well as the SHG and THG coefficients in asymmetric double n-type δ -doped GaAs QWs. We use the following values of the inverse of the lifetimes involved in the transitions: $\Gamma_1 = 1.0$ THz, $\Gamma_2 = 5.0$ THz, and $\Gamma_3 = 0.1$ THz [50]. The values chosen for ionized donor impurity concentrations $N_{2d}^{l,r}$ are $5.0 \times 10^{12} \text{ cm}^{-2}$ and $4.0 \times 10^{12} \text{ cm}^{-2}$ for the left- and right-hand δ -doped layer of impurities, respectively. The l_p value is set to 12 nm.

In Fig. 2 we report the behavior for the energy levels of the system as the in-plane (x-directed) magnetic field goes from zero until 40 T. Here we observe, as expected, that the energy levels rise as the magnetic field increases due to the field-induced increase of the confinement along the growth direction. This behavior is fundamental for the purpose of this study because it allows to increase the ISB energy level distance in such a way that we would be able to tune the optical properties of interest because they are related to the energy of the absorbed incident photon. Also there is an important connection to the dipole matrix element, which in this case strongly depends on the asymmetric shape of the confinement potential. As it was established in the Section 2, the calculation of the NOR coefficient requires only two energy levels, but this system has, at least, four confined energy levels in such a way that it is also feasible to compute the SHG that requires three energy level and the THG that needs an extra energy level. The potential profile studied here is, clearly, suitable for a response at this order of dielectric susceptibility. In accordance, in Fig. 3 we plot the energy levels differences for the main energy transition ($E_1 - E_0$), the half energy difference between the second excited state and the ground state ($E_2 - E_0$)/2; and finally ($E_3 - E_0$)/3 as a function of the applied magnetic field. In this figure we can observe that for values of B close to 10 T the values of $\omega_{20}/2$ and $\omega_{30}/3$ coincide, which produces an important signal for the third harmonic generation.

Fig. 4 shows the computed NOR coefficient for the system, plotted as a function of the incident photon energy, for several values of the applied magnetic field. As the NOR Eq. (11) dictates, this is a

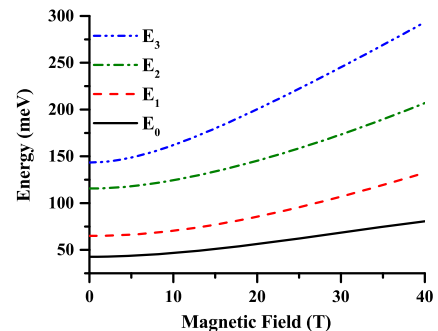


Fig. 2. The first four energy levels for an asymmetric double δ -doped GaAs quantum well as functions of the external, z-directed, applied magnetic field (B).

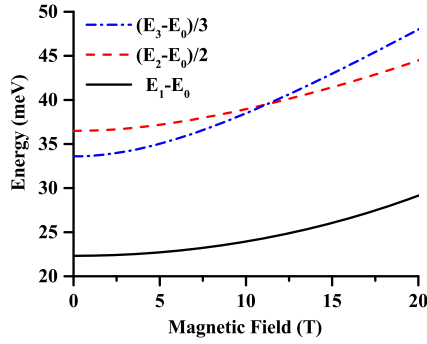


Fig. 3. Energy levels difference between the first-excited and ground state (solid line), second-excited and ground state, divided by 2 (dashed line), and third-excited state minus the ground state energy, divided by 3 (point-dashed line).

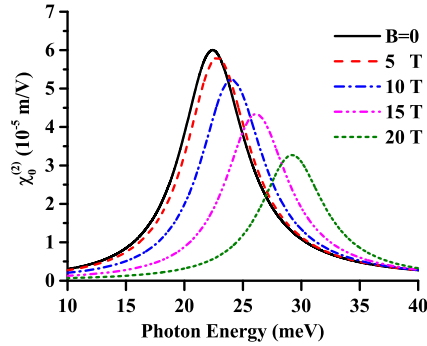


Fig. 4. The coefficient of nonlinear optical rectification for an asymmetric double δ -doped quantum well for several values of the applied magnetic field.

Lorentzian-like function that fundamentally depends of the natural frequency of the main energy transition $\omega_{10} = (E_1 - E_0)/\hbar$, of the dipole matrix element M_{01} as well as of the transition associated mean-electron-displacement δ_{01} . The other quantities are fixed parameters or well known physical quantities. We observe that the NOR exhibits a blueshift that can be clearly explained because ω_{10} increases as a function of the magnetic field (see Fig. 3). From Eq. (11) one may readily note that the magnitude of resonant peak of the NOR is proportional to the product $M_{01}^2 \delta_{01}$. As mentioned, as long as the magnetic field increases the separation between the energy levels grows. So, for larger B , the confinement potential becomes stronger and the confined states start to be more localized around $z = 0$. Consequently, the dipole matrix element M_{01} decreases. In addition, it is observed that with the increasing magnetic field the whole structure tends to be a symmetric parabolic quantum well with small perturbations in the bottom of the well. In the limit of high magnetic fields, the terms M_{11} and M_{00} tend simultaneously to zero, and so δ_{01} tends also to zero. For this particular configuration we find that for zero applied magnetic field, the maximum of the NOR is for an incident photon energy of about 22 meV and its magnitude is 6.0×10^{-5} m/V. When the magnetic field reaches 20 T, the maximum peak position is blue-shifted to an energy of about 29 meV while its magnitude falls almost 50% (3.2×10^{-5} m/V).

With regard to the SHG coefficient, results are depicted in Fig. 5. From Eq. (12), it is noticed that it depends on the double resonant frequencies ω_{20} and ω_{10} and on the product of dipole matrix elements $M_{01}M_{12}M_{20}$. The former depends on the intersubband energy levels separation and the latter is determined fundamentally by the wavefunction behavior. In particular, if the wavefunctions become spatially symmetric, the matrix element M_{20} is zero and the SHG also does. In the particular configuration studied here, for non-applied magnetic field, the first signal of the SHG is located at $\hbar \omega = 22$ meV and has magnitude of 0.46×10^{-6} m/V, while the second peak is for an incident photon energy of 36 meV and the signal is narrower, with an amplitude

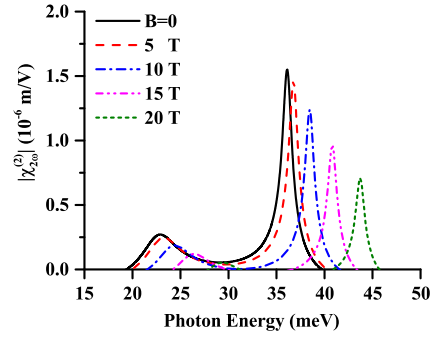


Fig. 5. The coefficient of Second Harmonic Generation (SHG) for an asymmetric double n-type δ -doped GaAs quantum well as a function of the incident photon energies with several magnetic field values.

of 1.81×10^{-6} m/V. In general, as the magnetic field is turned on for values 5, 10, 15, and 20 T, the first and second SHG-peaks experience a monotonic blue-shift as well as a diminishing in their maximum peak values. For instance, when the magnetic field is 20 T, the first (second) peak signal takes place for an incident photon energy of about 29 meV (44 meV) while its maximum magnitude is 0.46×10^{-6} m/V (0.91×10^{-6} m/V). It means that the SHG signals are blue-shifted about 15 meV and attenuated practically in 50% as the magnetic field goes from zero up to 20 T. In the particular case of magnetic field values here considered, the double resonant frequencies $\omega_{20}/2$ and ω_{10} does not coincide, consequently we do not have a single SHG peak. It is also important to stress that besides the wavefunctions does not become symmetric as B increases, the dipole matrix elements multiplication $M_{01}M_{12}M_{20}$ diminish monotonically because the field-induced modification of the confining potential along the growth direction reduces the contributions to the M_{ij} coming from larger values of z .

Finally, in Fig. 6 we are presenting the coefficient of THG ($\chi_{3\omega}^{(3)}$) as a function of the incident photon energy [see Eq. (13)]. Here one may observe that the THG depends upon the matrix element product $M_{01}M_{12}M_{23}M_{03}$ that, as in the case of SHG, can be zero if symmetric state wavefunctions are involved. In fact, a nonzero third-excited state to ground-state resonant frequency $\omega_{30} = (E_3 - E_0)/\hbar$, is the particular transition that, in our case, enables the THG in the system. In general we observe a blue-shift in the THG signal. For instance for zero and 5 T applied magnetic field the main peak of the THG is located at 33 and 35 meV, respectively. In particular for a magnetic field of 10 T, the THG exhibits an important peak, of maximum value of 7.4×10^{-12} m²/V², for an incident photon energy of about 39 meV. This peak corresponds to the situation when the energy differences $(E_3 - E_0)/3$ and $(E_2 - E_0)/2$ are almost equal, thus revealing the possibility of the field-induced tuning of this nonlinear optical response. Lastly, as the magnetic field further increases, the THG signal starts to vanish. Note that in all spectra, the resonant peak associated with $\hbar \omega = E_1 - E_0$ is absent. The main reason is that when

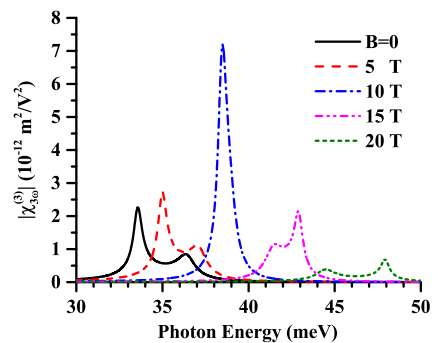


Fig. 6. The coefficient of Third Harmonic Generation (THG) for an asymmetric double n-type δ -doped GaAs quantum well as a function of the incident photon energy with several values of the applied magnetic field.

this condition is satisfied by the incident photon, the THG coefficient is proportional to the inverse of the product $\hbar^2(2\omega_{10} - \omega_{20} + i\Gamma_3/2)(3\omega_{10} - \omega_{30} + i\Gamma_3/3) \sim 10^3 \text{ meV}^2$ which is large enough to suppress the presence of the low energy resonant peak. When the photon energy coincides with the resonant condition of the main and secondary peaks, the factor associated with frequencies -which modulates the expectation values of the dipole- is of the order of hundreds of meV^2 , making the peaks visible in comparison with the low energy one. In all cases where the two structures appear, the main peak is associated with the transition $\hbar\omega = (E_3 - E_0)/3$ -the triple harmonics. The exchange of position between the main peak and the secondary one occurs at $B = 11.13 \text{ T}$ corresponding to the crossing between the differences $(E_2 - E_0)/2$ and $(E_3 - E_0)/3$ in the Fig. 3. Clearly the presence or absence of resonant peaks results from the competition between the dipole matrix elements and the energy differences between the involved states.

4. Conclusions

In this paper we report the coefficients NOR, SHG, and THG for an asymmetric double n-type δ -doped quantum well in GaAs, taking into account the application of an in-plane (x -directed) magnetic field. In general, it is concluded that the NOR, SHG, and THG nonlinear responses can be suitably controlled by this externally applied magnetic field. In particular, the NOR experiences a blue-shift with amplitude-decreased as long as the field strengths augments. The same behavior holds for the SHG, but not for the THG. Instead, as the magnetic field increases from zero up to 20 the coefficient of this particular property exhibits a well defined THG signal for a magnetic field value about 10 T. We find that for the chosen configuration the harmonics generation occur in the far-infrared region (or, more properly speaking, from several to few tens of THz in the frequency interval) and, therefore, these quantum structures could be suitable building blocks for photodetectors in this range of the electromagnetic spectra.

Acknowledgements

This research was partially supported by the “Programa de Fortalecimiento de la Calidad en Instituciones Educativas (SEP)” with project “Fortalecimiento y consolidación de los PE y los CA de la DES de Ciencias Básicas de la Universidad Autónoma de Zacatecas”. This research was also partially supported by Colombian Agencies: CODI-Universidad de Antioquia (Estrategia de Sostenibilidad de la Universidad de Antioquia) and Facultad de Ciencias Exactas y Naturales-Universidad de Antioquia (CAD dedication projects 2016-2017). K.A. R.-M. and J.G. R.-B would like to acknowledges to CONACyT- México for the financial support through grants 275399 and 275402.

References

- [1] J. Singh, *Electronic and Optoelectronic Properties of Semiconductor Structures*, first edition, Cambridge University Press, 2003.
- [2] P. Yu, M. Cardona, *Fundamentals of Semiconductors*, fourth edition, Springer, 2010.
- [3] A. Rajira, H. Akabli, A. Almaggousi, A. Abounadi, The non parabolicity and the enhancement of the intersubband absorption in GaAs/GaAlAs quantum wells, *Superlattice Microstruct.* 84 (2015) 192. <http://dx.doi.org/10.1016/j.spmi.2015.05.008>.
- [4] M. Msahli, H. Saidi, A.B. Ahmed, S. Ridene, H. Bouchriha, Oscillator strengths for the intersubband transitions in GaAs/InGa_{1-x}As quantum wells and its strain dependence, *Optik* 127 (2016) 4903. <http://dx.doi.org/10.1016/j.ijleo.2016.01.202>.
- [5] D. Liu, Y. Cheng, J. He, Hot-phonon effect on intersubband absorption in GaN/AlGaN quantum well structures, *Superlattice Microstruct.* 89 (2016) 362. <http://dx.doi.org/10.1016/j.spmi.2015.11.034>.
- [6] S.-H. Park, D. Ahn, C.-Y. Park, Intersubband absorption coefficients of GaN/AlN and strain-compensated InGaN/InAlN quantum well structures, *Superlattice Microstruct.* 100 (2016) 508. <http://dx.doi.org/10.1016/j.spmi.2016.10.001>.
- [7] D. Liu, E.X. Wang, K. Guo, Influence of thin AlAs layer insertion on intersubband optical transitions in GaAs/AlGaAs quantum-well structures, *Physica E* 86 (2017) 64. <http://dx.doi.org/10.1016/j.physe.2016.10.008>.
- [8] E. Ozturk, I. Sokmen, Intersubband transitions in an asymmetric double quantum well, *Superlattice Microstruct.* 41 (2007) 36. <http://dx.doi.org/10.1016/j.spmi.2006.10.006>.
- [9] E. Ozturk, I. Sokmen, Effect of magnetic fields on the linear and nonlinear intersubband optical absorption coefficients and refractive index changes in square and graded quantum wells, *Superlattice Microstruct.* 48 (2010) 312. <http://dx.doi.org/10.1016/j.spmi.2010.06.015>.
- [10] U. Yesilgul, E.B. Al, J.C. Martínez-Orozco, R.L. Restrepo, M.E. Mora-Ramos, C.A. Duque, F. Ungan, E. Kasapoglu, Linear and nonlinear optical properties in an asymmetric double quantum well under intense laser field: effects of applied electric and magnetic fields, *Opt. Mater.* 58 (2016) 107. <http://dx.doi.org/10.1016/j.optmat.2016.03.043>.
- [11] R.L. Restrepo, G.L. Miranda, C.A. Duque, M.E. Mora-Ramos, Simultaneous effects of hydrostatic pressure and applied electric field on the impurity-related self-polarization in GaAs - Ga_{1-x}Al_xAs multiple quantum wells, *J. Lumin.* 131 (2011) 1016. <http://dx.doi.org/10.1016/j.jlumin.2011.01.014>.
- [12] Í. Karabulut, C.A. Duque, Nonlinear optical rectification and optical absorption in GaAs - Ga_{1-x}Al_xAs double quantum wells under applied electric and magnetic fields, *Physica E* 43 (2011) 1405. <http://dx.doi.org/10.1016/j.physe.2011.03.013>.
- [13] G.L. Miranda, M.E. Mora-Ramos, C.A. Duque, Exciton-related energies of the 1s-like states of excitons in GaAs - Ga_{1-x}Al_xAs double quantum wells, *J. Lumin.* 132 (2012) 2525. <http://dx.doi.org/10.1016/j.jlumin.2012.05.015>.
- [14] G.L. Miranda, M.E. Mora-Ramos, C.A. Duque, Exciton-related nonlinear optical absorption and refractive index change in GaAs-Ga_{1-x}Al_xAs double quantum wells, *Physica B* 409 (2013) 78. <http://dx.doi.org/10.1016/j.physb.2012.10.008>.
- [15] S. Das, R.K. Nayak, T. Sahu, A.K. Panda, Enhancement of electron mobility in asymmetric coupled quantum well structures, *J. Appl. Phys.* 115 (2014) 073701. <http://dx.doi.org/10.1063/1.4865877>.
- [16] G. Rezaei, M.J. Karimi, A. Keshavarz, Excitonic effects on the nonlinear intersubband optical properties of a semi-parabolic one-dimensional quantum dot, *Physica E* 43 (2010) 475. <http://dx.doi.org/10.1016/j.physe.2010.08.035>.
- [17] M.J. Karimi, G. Rezaei, Effects of external electric and magnetic fields on the linear and nonlinear intersubband optical properties of finite semi-parabolic quantum dots, *Physica B* 406 (2011) 4423. <http://dx.doi.org/10.1016/j.physb.2011.08.105>.
- [18] X.Q. Yu, Y.B. Yu, Optical absorptions in asymmetrical semi-parabolic quantum wells, *Superlattice Microstruct.* 62 (2013) 225. <http://dx.doi.org/10.1016/j.spmi.2013.07.021>.
- [19] H.V. Phuc, L.V. Tung, Linear and nonlinear phonon-assisted cyclotron resonances in parabolic quantum well under the applied electric field, *Superlattice Microstruct.* 71 (2014) 124. <http://dx.doi.org/10.1016/j.spmi.2014.03.022>.
- [20] U. Yesilgul, F. Ungan, S. Sakiroglu, M.E. Mora-Ramos, C.A. Duque, E. Kasapoglu, H. Sari, I. Sökmen, Effect of intense high-frequency laser field on the linear and nonlinear intersubband optical absorption coefficients and refractive index changes in a parabolic quantum well under the applied electric field, *J. Lumin.* 145 (2014) 379. <http://dx.doi.org/10.1016/j.jlumin.2013.07.062>.
- [21] F. Ungan, J.C. Martínez-Orozco, R.L. Restrepo, M.E. Mora-Ramos, E. Kasapoglu, C.A. Duque, Nonlinear optical rectification and second-harmonic generation in a semi-parabolic quantum well under intense laser field: effects of electric and magnetic fields, *Superlattice Microstruct.* 81 (2015) 26. <http://dx.doi.org/10.1016/j.spmi.2015.01.016>.
- [22] S. Panda, B.K. Panda, Optical properties in symmetric and asymmetric pöschl-teller potentials under intense laser field, *Superlattice Microstruct.* 73 (2014) 160. <http://dx.doi.org/10.1016/j.spmi.2013.11.001>.
- [23] T.F. Kuech, S.E. Babcock, L. Mawst, Growth far from equilibrium: examples from III-V semiconductors, *Appl. Phys. Rev.* 3 (2016) 040801. <http://dx.doi.org/10.1063/1.4944801>.
- [24] E. Rosencher, P. Bois, J. Nagle, E. Costard, S. Delaitre, Observation of nonlinear optical rectification at 10.6 μm in compositionally asymmetrical algaas multi-quantum wells, *Appl. Phys. Lett.* 55 (1989) 1597. <http://dx.doi.org/10.1063/1.102248>.
- [25] L. Tsang, D. Ahn, S.L. Chuang, Electric field control of optical second-harmonic generation in a quantum well, *Appl. Phys. Lett.* 52 (1988) 697. <http://dx.doi.org/10.1063/1.99350>.
- [26] R. Camacho-Morales, M. Rahmani, S. Kruk, L. Wang, L. Xu, D.A. Smirnova, A.S. Solntsev, A. Miroshnichenko, H.H. Tan, F. Karouta, S. Naureen, K. Vora, L. Carletti, C. De Angelis, C. Jagadish, Y.S. Kivshar, D.N. Neshev, Nonlinear generation of vector beams from AlGaAs nanoantennas, *Nano Lett.* 16 (2016) 7191. <http://dx.doi.org/10.1021/acs.nanolett.6b03525>.
- [27] D.P. Davé, Enhanced field control of second harmonic generation in compositionally asymmetrical quantum wells, *J. Appl. Phys.* 75 (1994) 8222. <http://dx.doi.org/10.1063/1.356527>.
- [28] S. Campione, A. Benz, M.B. Sinclair, F. Capolino, I. Brener, Second harmonic generation from metamaterials strongly coupled to intersubband transitions in quantum wells, *Appl. Phys. Lett.* 104 (2014) 131104. <http://dx.doi.org/10.1063/1.4870072>.
- [29] R.-Z. Wang, K.-X. Guo, B. Chen, Y.-B. Zheng, B. Li, Third-harmonic generation in asymmetric coupled quantum wells, *Superlattice Microstruct.* 45 (2009) 8. <http://dx.doi.org/10.1016/j.spmi.2008.10.011>.
- [30] L. Zhang, H.-J. Xie, Bound states and third-harmonic generation in a semi-parabolic quantum well with an applied electric field, *Physica E* 22 (2004) 791. <http://dx.doi.org/10.1016/j.physe.2003.08.001>.
- [31] J. Ganguly, S. Saha, S. Pal, M. Ghosh, Fabricating third-order nonlinear optical susceptibility of impurity doped quantum dots in the presence of gaussian white noise, *Opt. Commun.* 363 (2016) 47. <http://dx.doi.org/10.1016/j.opt->

- com.2015.10.052.
- [32] N. Zeiri, N. Sfina, S.A.-B. Nasrallah, J.-L. Lazzari, M. Said, Intersubband transitions in quantum well mid-infrared photodetectors, *Infrared Phys. Technol.* 60 (2013) 137. <http://dx.doi.org/10.1016/j.infrared.2013.04.004>.
- [33] M. Zavvari, K. Abedi, A. Yuseffi, M. Karimi, Proposal of a quantum ring intersubband photodetector integrated with avalanche multiplication region for high performance detection of far infrared, *Optik* 126 (2015) 1861. <http://dx.doi.org/10.1016/j.ijleo.2015.05.013>.
- [34] E. Ozturk, I. Sokmen, Intersubband optical absorption of double Si δ -doped GaAs layers, *Superlattice Microstruct.* 35 (2004) 95. <http://dx.doi.org/10.1016/j.spmi.2004.02.020>.
- [35] E. Ozturk, Optical intersubband transitions in double Si δ -doped GaAs under an applied magnetic field, *Superlattice Microstruct.* 46 (2009) 752. <http://dx.doi.org/10.1016/j.spmi.2009.07.013>.
- [36] J.C. Martínez-Orozco, M.E. Mora-Ramos, C.A. Duque, Nonlinear optical rectification and second and third harmonic generation in GaAs δ -FET systems under hydrostatic pressure, *J. Lumin.* 132 (2012) 449. <http://dx.doi.org/10.1016/j.jlumin.2011.09.020>.
- [37] O. Oubram, O. Navarro, L.M. Gaggero-Sager, J.C. Martínez-Orozco, I. Rodríguez-Vargas, The hydrostatic pressure effects on intersubband optical absorption of n-type δ -doped quantum well in GaAs, *Solid State Sci.* 14 (2012) 440. <http://dx.doi.org/10.1016/j.solidstatesciences.2012.01.020>.
- [38] M.E. Mora-Ramos, L.M. Gaggero-Sager, C.A. Duque, Binding energy of a donor impurity in GaAs δ -doped systems under electric and magnetic fields, and hydrostatic pressure, *Physica E* 44 (2012) 1335. <http://dx.doi.org/10.1016/j.physe.2012.02.014>.
- [39] J.C. Martínez-Orozco, M.E. Mora-Ramos, C.A. Duque, The nonlinear optical absorption and corrections to the refractive index in a GaAs n-type delta-doped field effect transistor under hydrostatic pressure, *Phys. Status Solidi B* 249 (2012) 146. <http://dx.doi.org/10.1002/pssb.201147301>.
- [40] J.G. Rojas-Briseño, J.C. Martínez-Orozco, I. Rodríguez-Vargas, M.E. Mora-Ramos, C.A. Duque, Nonlinear absorption coefficient and relative refraction index change for an asymmetrical double δ -doped quantum well in GaAs with a Schottky barrier potential, *Physica B* 424 (2013) 13. <http://dx.doi.org/10.1016/j.physb.2013.05.004>.
- [41] K.A. Rodríguez-Magdaleno, J.C. Martínez-Orozco, I. Rodríguez-Vargas, M.E. Mora-Ramos, C.A. Duque, Asymmetric GaAs n-type double δ -doped quantum wells as a source of intersubband-related nonlinear optical response: effects of an applied electric field, *J. Lumin.* 147 (2014) 77. <http://dx.doi.org/10.1016/j.jlumin.2013.10.057>.
- [42] J.G. Rojas-Briseño, J.C. Martínez-Orozco, I. Rodríguez-Vargas, M.E. Mora-Ramos, C.A. Duque, Nonlinear optical properties in an asymmetric double δ -doped quantum well with a Schottky barrier: electric field effects, *Phys. Status Solidi (b)* 251 (2014) 415. <http://dx.doi.org/10.1002/pssb.201350050>.
- [43] C.A. Duque, V. Akimov, R. Demediuk, V. Belykh, A. Tiutiunnyk, A.L. Morales, R.L. Restrepo, M.E. Mora-Ramos, O. Fomina, V. Tulupenko, Intersubband linear and nonlinear optical response of the delta-doped SiGe quantum well, *Superlattice Microstruct.* 87 (2015) 125. <http://dx.doi.org/10.1016/j.spmi.2015.05.039>.
- [44] E. Ozturk, Y. Ozdemir, Linear and nonlinear intersubband optical absorption coefficient and refractive index change in n-type δ -doped GaAs structure, *Opt. Commun.* 294 (2013) 361. <http://dx.doi.org/10.1016/j.optcom.2012.12.035>.
- [45] G. Gumbs, Self-consistent density of states for a single- and double-quantum-well structure in a parallel magnetic field, *Phys. Rev. B* 54 (1996) 11354. <http://dx.doi.org/10.1103/PhysRevB.54.11354>.
- [46] L. Ioriatti, Thomas-Fermi theory of δ -doped semiconductor structures: exact analytical results in the high-density limit, *Phys. Rev. B* 41 (1990) 8340. <http://dx.doi.org/10.1103/PhysRevB.41.8340>.
- [47] E. Rosencher, P. Bois, Model system for optical nonlinearities: asymmetric quantum wells, *Phys. Rev. B* 44 (1991) 11315. <http://dx.doi.org/10.1103/PhysRevB.44.11315>.
- [48] S. Shao, K.-X. Guo, Z.-H. Zhang, N. Li, C. Peng, Third-harmonic generation in cylindrical quantum dots in a static magnetic field, *Solid. State Commun.* 151 (2011) 289. <http://dx.doi.org/10.1016/j.ssc.2010.12.003>.
- [49] Jian-Hui Yuan, Ni Chen, Zhi-Hai Zhang, Jing Su, Su-Fang Zhou, Xiao-ling Lu, Yong-Xiang Zhao, Energy spectra and the third-order nonlinear optical properties in GaAs/AlGaAs core/shell quantum dots with a hydrogenic impurity, *Superlattices Microstruct.* 100 (2016) 957. <http://dx.doi.org/10.1016/j.spmi.2016.10.068>.
- [50] G. Wang, K. Guo, Excitonic effects on the third-harmonic generation in parabolic quantum dots, *J. Phys.-Condens. Matter* 13 (2001) 8197. <http://dx.doi.org/10.1088/0953-8984/13/35/324>.